Interplay of fluvial incision and rockfalls in shaping periglacial mountain gorges

Thibaut Cardinal [a,*], Laurence Audin [b], Yann Rolland [c], Stéphane Schwartz [b], Carole Petit [a], Swann Zerathe [b], Laurent Borgniet [d], Régis Braucher [e], Jérôme Nomade [b], Thierry Dumont [b], Valery Guillou [e], ASTER team [e,1]

[a] Université Côte d'Azur, CNRS, Observatoire de la Côte d'Azur, IRD, Géoazur, F-06560 Valbonne, France
[b] Université Grenoble Alpes, Université Savoie Mont Blanc, CNRS, IRD, IFSTTAR, ISTerre, 38000 Grenoble, France
[c] Université Savoie Mont Blanc, CNRS, Pôle Montagne, Edytem, F-73370 Le Bourget-du-Lac, France
[d] Université Grenoble Alpes, INRAE, LESSEM, F-38000 Grenoble, France
[e] CEREGE, Aix-Marseille Univ., CNRS, IRD, Coll. de France, INRAE, Technopôle de l'Environnement Arbois-Méditerranée, BP80, 13545 Aix-en-Provence, France

ARTICLE INFO

ABSTRACT

Fluvial incision is the consequence of landscape readjustment to combined tectonic and climatic processes. In the southwestern Alps (Haute Provence Geopark), deep gorges incised by the Bès River attest of efficient erosional processes at the front of the Alpine mountain range. This catchment stands in a peripheral Alpine position, out of the glaciated domain during the last glacial periods, which makes it suitable to quantify fluvial incision and related erosional processes in a glacier-free environment. In this paper, we combine high resolution 3D topographic mapping and in situ produced cosmogenic ^{36}Cl dating of a mountain gorge (the "Clue de Barles" Gorge). First, the very high-resolution 3D topographic modeling from aerial and drone surveys permits to map the erosion markers on the gorge walls and to accurately determine the topographic shielding factor for Cosmic Ray Exposure (CRE) dating. Secondly, ^{36}Cl CRE age distribution highlights two distinct geomorphic domains along the vertical profile: i) the higher section is characterized by clusters of similar CRE ages, interpreted as related to paraglacial rockfall events; ii) the lower section shows increasing ages with height, which are ascribed to fluvial incision occurring at a rate of 0.15 mm/yr since 25 ka, and of 2 mm/yr since 2 ka. Our results for the Clue de Barles, compared to other sites in the South French Alps highlight that: i) the gorge morphology is the result of the combination of both vertical fluvial incision and lateral gravitational processes, ii) the mean Quaternary fluvial incision rate in the Bès River catchment is at least twice lower than further east in the formerly glaciated Alps.

1. Introduction

The erosive response of landscapes through times provides a record of the interaction between lithospheric and atmospheric forcing. The lithospheric forcing comprises isostatic readjustment and tectonic motions (England and Molnar, 1990; Lavé and Avouac, 2001; Wobus et al., 2006), while the atmospheric forcing consists of local or global climate variations (Van der Woerd et al., 2002; Pan et al., 2003; Bacon et al., 2009). Fluvial, glacial and gravitational erosion processes play a significant role in the shaping of the landforms in an "erosion-uplift" self-balancing system (Adams, 1985). River dynamics therefore provide

quantitative information on landscape evolution because their morphology and erosive power are directly linked to processes that can affect landforms: tectonic, mass movements, climate change (Pratt et al., 2002; Kirby and Whipple, 2012).

The study of fluvial landscapes evolution relies on available Quaternary geomorphological markers such as terraces and incised river gorges (Pazzaglia et al., 1998; Saillard et al., 2014; Rolland et al., 2017). However, processes that led to the formation of these geomorphological objects are often poorly quantified when it comes to vertical markers. Indeed, these 3D morphologies record a combination of different mechanisms such as fluvial incision, gravitational destabilization, like landslides or rockfalls, or glacier advances related to late glacial episodes (Whipple et al., 1999; Brocklehurst and Whipple, 2002; Montgomery, 2002; Brocard et al., 2003; Valla et al., 2011). Quaternary geomorphological shaping of the Alpine belt and the evolution of landforms are generally explained by the alternation of glacial and inter-glacial phases, which produce significant vertical uplift after each deglaciation (Champagnac et al., 2007, 2008; Valla et al., 2010) and lead to a strong bedrock incision by the river network. The formation

---

of peculiar fluvial markers, like bedrock gorges (named in local French language "clues" when the river runs perpendicular to the bedding), marked by deeply incised rock walls have been variously interpreted as features typical of sub-glacial incisions (Korup and Schlunegger, 2007; Montgomery and Korup, 2010) or of fluvial incision of the Late Quaternary (Saillard et al., 2014; Rolland et al., 2017; Petit et al., 2017, 2019). In all these studies, the contribution of rockfall events has never been put forward as an efficient process for the long-term shaping of mountain gorges. These investigated catchments have headwaters located in high altitude massifs, under the influence of glaciers since the Late Glacial Maximum (LGM), which led to efficient fluvial incision during deglaciation. For all these investigated sites, the CRE data evidenced a strong relation between the onset of incision and the post-LGM deglaciation, which led these authors to propose that climatic variations are the major external factor responsible for the incision through punctual but strong glacial outburst floods during interglacials (e.g. Petit et al., 2017; Rolland et al., 2017).

In this paper, we focus on the Clue de Barles (CdB) Gorge in southwestern Alps (Southern French Alps). The site is located at the front of the subalpine fold and thrust belt, in the Bès Valley (Fig. 1A and B), which catchment has likely been disconnected from any significant glacial influence during the LGM (Brisset et al., 2015 and references therein). This valley is currently at the boundary between the stable Alpine foreland and the actively uplifting chain, as detected by vertical GPS measurements (>0.5 mm/yr; Serpelloni et al., 2013; Nocquet et al., 2016; Sternai et al., 2019). It thus appears as a key area to determine the response of a catchment unaffected by glaciers influence and undergoing a slow uplift.

In this paper, we aim to highlight the different erosive processes that lead to the gorge formation in a fluvial-dominated catchment, based on the acquisition of a high-resolution Digital Elevation Model (DEM) of the CdB Gorge and its related environment and a high-resolution CRE dating profile of the ~100 m high, nearly vertical gorge walls. These new data allow us to assess the relative contribution of gravitational and fluvial incision processes in the shaping of gorges along an apparently smooth profile. Finally, we compare these data with previous studies available along different catchments in the Alpine foreland after the LGM.

2. Geological and geomorphic setting

2.1. Geological setting: the Barles erosional "half-window"

Our geomorphic target, the Clue de Barles (CdB) Gorge, is located in the foreland of the southwestern Alps (Fig. 1A). This fold-and-thrust belt has undergone tectonic shortening in Cenozoic times due to the Alpine collision (Dumont et al., 2012; Schwartz et al., 2017). The geological structure of the region comprises the Digne nappe, made of a thick Early Jurassic limestone and marl series in the study area, which was thrust over onto the Cenozoic foreland molassic basin presently outcropping in an erosional half-window: the Barles "half-window" in the Digne Geopark (Fig. 1B; Hippolyte and Dumont, 2000). At the present time, the region is still undergoing active but very slow deformation, under a compressive tectonic context (Sue et al., 2007), as shown by geodesy (Walpersdorf et al., 2018) and seismicity (Delacou et al., 2004).

In the study area, erosion due to the Bès River, a tributary of the Durance River, has participated to the formation of the erosional half-window (Fig. 1B) revealing the folded and faulted sedimentary cover in the foreland beneath the Digne Nappe (Fig. 1C). The formation of this erosional feature is related to tectonic uplift controlled by Pliocene crustal thickening (Schwartz et al., 2017). Thermochronological inversion modeling by Schwartz et al. (2017) showed that the onset of the
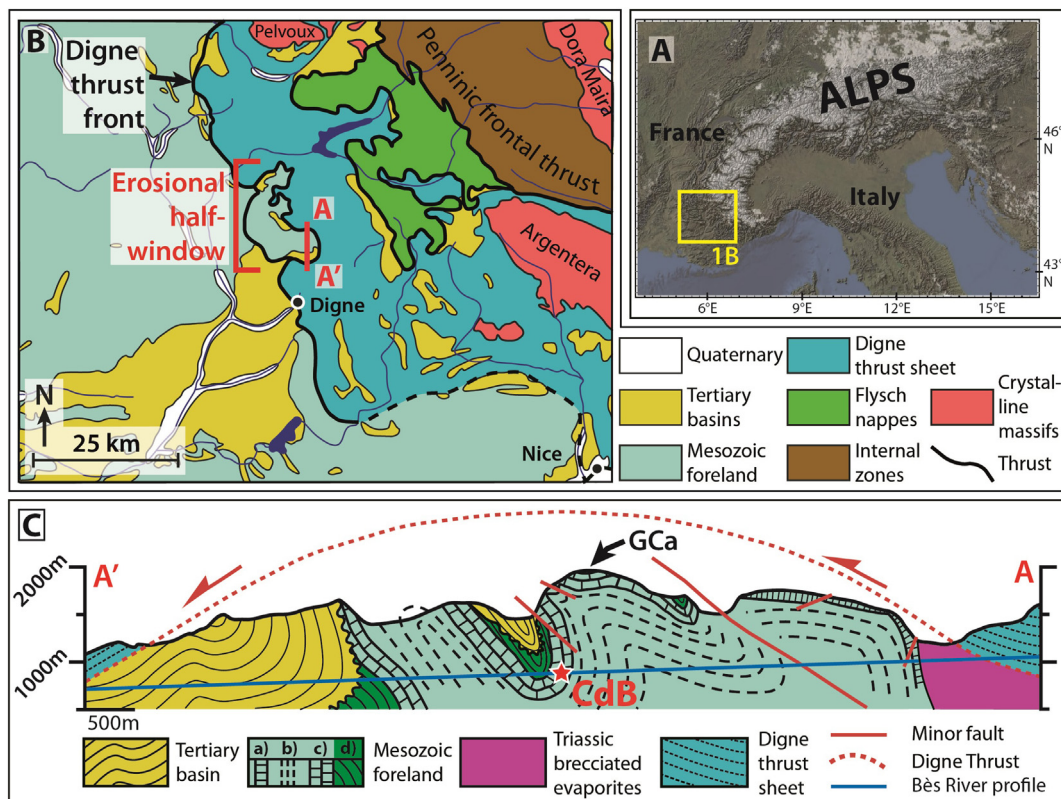

Fig. 1. A, Location of study area in the European Alps. B, Location of the Barles half-window in the Western Alps general tectonic framework (modified from Schwartz et al., 2017). C, Geological cross-section of the Barles erosional half-window along the Bès River profile. Mesozoic foreland a) massive Early Jurassic; b) Middle to Late Jurassic "Terres Noires"; c) Late Jurassic "Tithonian limestones"; d) Cretaceous. Note the folding of the Tithonian limestones that form the Grande Cloche anticline (GCa) in which the Clue de Barles Gorges (red star; CdB) is dug by the Bès River.

half-window exhumation began at 6 Ma (with a denudation rate of ≈0.7 mm/yr). Since then, erosion, in response to the tectonic uplift (Fig. 1C), has removed up to 4 km of the Digne nappe cover.

2.2. Geomorphological setting

The diversity of landscape morphologies in the Bès Valley is partly explained by differential erosion due to the strong lithological variations between marly and carbonate rich formations. Indeed, wide, smooth and open valleys shaped by landslides and gully dynamics are observed in Middle Jurassic shales locally named the "Terres Noires formation" (Fig. 2A). These low relief areas are delineated by adjacent strata of much more competent Late Jurassic limestones. The Terres Noires formation is exposed in the core of anticlines while the synclines preserve Cretaceous strata, as well as Oligocene to Miocene molassic deposits unconformably lying over the Mesozoic sequence (Fig. 1C). The absence of any glacial geomorphological markers, such as moraines or U-shaped valleys, precludes any significant glacial erosion in the Bès catchment during the LGM, as also documented by studies on the maximum glacial extension in the SW Alps (Brisset et al., 2015 and references therein). Recent incision of the Late Jurassic limestones (up to 250 m thick) by

the Bès River has shaped the CdB Gorge in the southern flank of the overturned "Grande Cloche" anticline (GCa; Figs. 1C and 2A).

Fig. 2 presents three different domains along the gorge perpendicular profile:

1) sub-horizontal surfaces above the gorge,
2) steep slopes of the two gorge walls facing each other that are widening as the altitude increases, reaching ≈150 m of width at ≈150 m high above the river level,
3) sub-vertical river polished walls that form a narrow incision canyon in the lowest part (≈10 m high above river level) (Fig. 2B, C and D).

The V-shaped profile of the gorge suggests that at larger scale its morphology may not only be controlled by fluvial incision, but also by lateral erosional processes affecting the gorge walls as the Bès River incises vertically.

3. Methods

3.1. Strategy and sampling

Gorge walls are theoretically gradually exposed during the incision process (Schaller et al., 2005; Ouimet et al., 2008). Therefore,
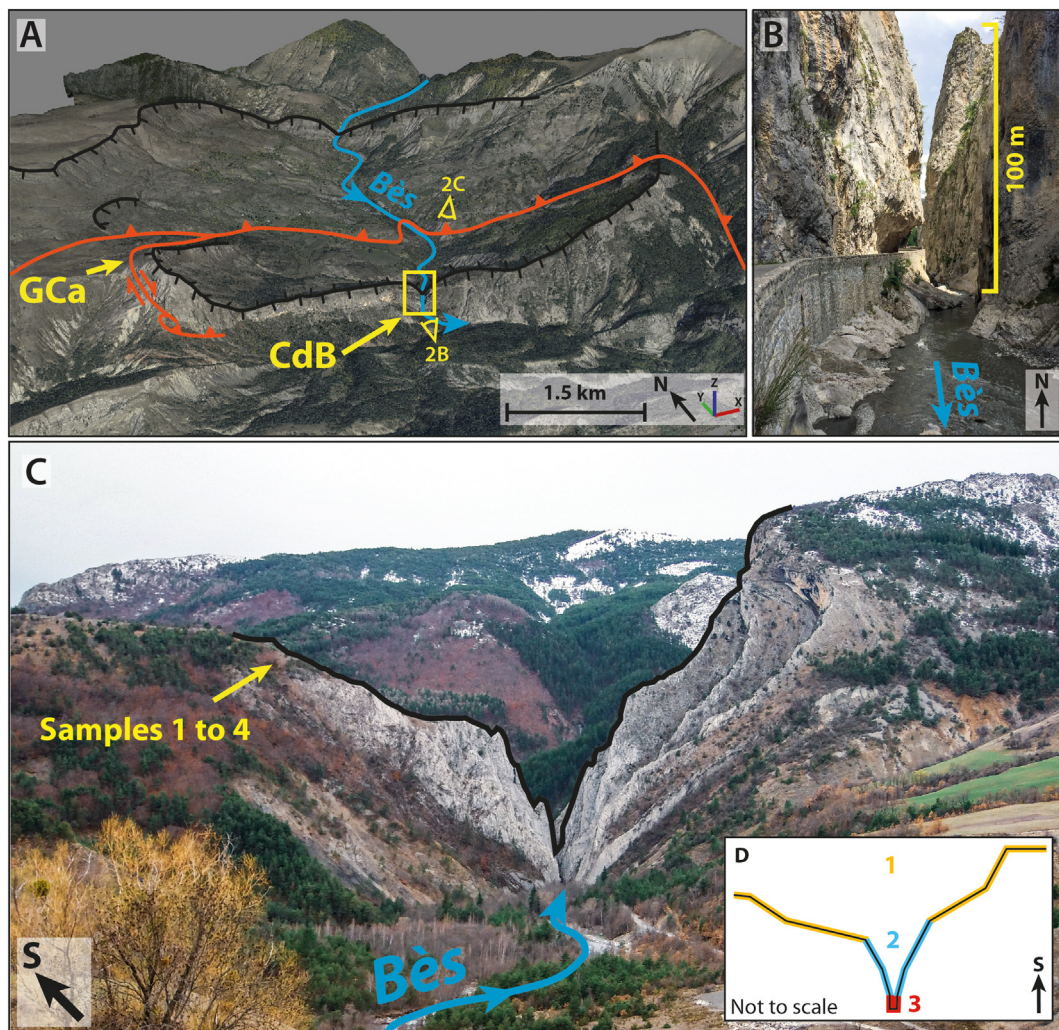

Fig. 2. A, Digital Elevation Model (DEM) based 3D view from the of the study area featuring the incised limestone bars (thick black lines) north and south of a large open valley. B, Terrestrial photographs of the Clue de Barles (CdB) Gorge. C, Panoramic view of the CdB Gorge towards the South featuring the vertical Tithonian limestone strata. Note the V shaped lateral profile of the gorge, highlighted on the photographs (black thick line). D, schematic interpretation of the V shaped profile of the gorge showing the 3 different domains: 1) sub-horizontal surfaces above the gorge, 2) steep slopes of the two gorge walls facing each other that are widening as the altitude increases, reaching ≈150 m of width at ≈150 m high above the river level, 3) sub-vertical river polished walls that form a narrow incision in the lowest part (≈10 m high).

cosmogenic radionuclide exposure (CRE) dating of the gorge wall should reveal a systematic rejuvenation of the CRE ages towards the current riverbed level through a correlation between the altitude of the samples and their CRE age. However, gravitational processes, like rockfall events, may also cause the rejuvenation of a gorge wall surface. If the wall compartment involved in a rockfall event is thicker than ≈2 m, the resulting exposed surface should not retain any cosmogenic inheritance prior to the gravitational event, as ≈95% of the cosmic radiation is absorbed in the first 1.8 m below the surface (Lal, 1991). Hence its concentration in cosmogenic nuclides should be null at the time of the rockfall, and subsequently, the CRE age should correspond to that of the gravitational event. Therefore, cosmogenic radionuclide concentration measurement is a well suited dating method to obtain chronological information of both gravitational and fluvial processes, and thus allows dating rockfall events and quantifying incision rate on the same spot.

Sampled surfaces were chosen for incision rate estimation, based on the following morphological indices: i) a surface with evidence of induration varnish or with low apparent superficial dissolution, indicating little erosion since exposure or ii) vicinity to peculiar concave erosional surfaces ("pot holes") preserved in the gorge walls that points to the last stalling point before the incision phase. The identification of such markers and the necessity to avoid samples with a too large topographic shielding led to the choice of a ≈10 m high, well-preserved wall located at the southern (i.e., downstream) extremity of the gorge (Fig. 3). The dissolution, weathering patina and superficial smoothing of the limestone surface of the gorge prevented us from confidently identifying a priori gravitational markers from the wall morphology through field and DEM based observations, by any rockfall scars characterized by edged surface and distinct coloration due to the lack of patina. We then chose to sample regularly the ≈70 m high wall rising above the preserved surface along a sub-vertical profile (Fig. 3A and C).

Along this profile, twenty limestone samples were collected, using a drill, hammer and chisel. The sampled surfaces include the lower and preserved river-polished surface and the upper slightly widening part of the gorge wall. In total, the gorge profile extends from the river up to 80 m high on two parallel vertical limestone strata (Fig. 3C). We sampled surfaces with no overhanging relief to minimize the topographic shielding and to simplify the topographic shielding factor determination.

In parallel, four samples were collected on the eastern sub-horizontal top of the limestone bar overlooking the gorge to constrain the local denudation rate in this part of the catchment (Figs. 2C and 3A).

3.2. Analytical protocol

Samples were prepared at the Laboratoire National des Nucléides Cosmogéniques (LN2C; CEREGE, Aix-en-Provence) following the procedure presented by Schimmelpfennig et al. (2009). ^{36}Cl concentrations were determined by accelerator mass spectrometry (AMS) performed on ASTER, the French national AMS facility (CEREGE, Aix en Provence) (Arnold et al., 2010). All measurements were calibrated against in-House CEREGE SM-CL-12 standard (Merchel et al., 2011). Total uncertainties account for counting statistics, standard evolution during measurements, standard uncertainty and external uncertainties of 2.74%, 2.13% and 1.62% for ^{36}Cl/^{35}Cl, 36Cl/37Cl and ^{35}Cl/^{37}Cl ratios, respectively (Braucher et al., 2018). The full chemical compositions of the two sampled Tithonian limestone strata were analyzed at CRPG (Nancy) in order to take into account the various ^{36}Cl production pathways (Schimmelpfennig et al., 2009). A sea level and high latitude ^{36}Cl production rate for calcium spallation of 42.2 ± 3.4 atoms ^{36}Cl g^{-1} yr^{-1} (Schimmelpfennig et al., 2009; Braucher et al., 2011) has been used and scaled after Stone (2000) and corrected for topographic shielding (see next paragraph). ^{36}Cl ages have been determined using the approach of Schimmelpfennig et al. (2009) using a limestone density of 2.6 g·cm^{-3}. CRE data are displayed in Table 1.

Topographic shielding was first determined from field data. Furthermore, we chose to use a high resolution DEM, built from a drone survey of the gorge and its surroundings, in order to be able to precisely recalculate the shielding parameters on each sampled surface.
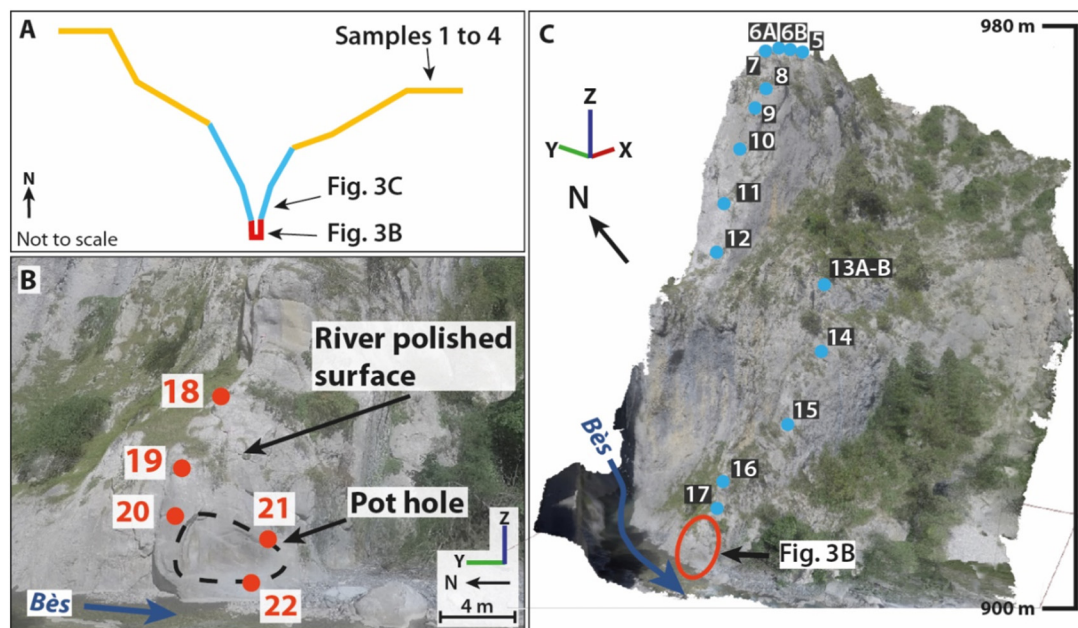

Fig. 3. A, schematic interpretation of the gorge V shaped profile and location of the sample gathered for CRE dating. B, Digital Elevation Model (DEM) based 3D view of the lower part of the sampling profile and location of the corresponding samples (18 to 20). Note the presence of a "pot hole" that indicates the preserved nature of the river polished sampled surface. Above sample 18, the preservation of the fluvial polished surface on the gorge wall is not sure and might have suffer post-incision erosion processes (dissolution and/or gravitational processes). C, All samples located on the high-resolution 3D DEM of the 80 m high CdB Gorge wall.

Table 1
^{36}Cl CRE sample characteristics and geochronological data. Sample field information, natural chlorine, calcium, and cosmogenic ^{36}Cl contents in the limestone samples and resulting ^{36}Cl CRE ages and denudation rates, TS factor and strike and dip of the sampled surfaces are indicated.

Sample	Altitude above sea level (m)	Height above river (m)	Lat	Long	Spall. scaling	^{35}Cl (ppm)	Ca (%)	Atoms ^{36}Cl (at/g)	Atoms ^{36}Cl uncertainty (at/g)	CRE age (yr)	Denudation rate (mm/ka)	TS factor	Surface strike and dip
1	1165.0	263.0	44.23	6.26	2.64	60.5	36.0	18,885,474	111,338	–	32.83 ± 1.94	0.99	Sub-horizontal
2	1155.6	253.6	44.23	6.26	2.62	48.5	39.0	2,767,824	155,686	–	18.74 ± 1.05	0.99	Sub-horizontal
3	1151.7	249.7	44.23	6.26	2.61	81.3	38.2	2,844,314	195,423	–	22.91 ± 1.57	0.99	Sub-horizontal
4	1154.9	252.9	44.23	6.26	2.62	38.0	31.9	1,563,115	84,417	–	32.54 ± 1.76	0.99	Sub-horizontal
5	975.2	73.2	44.23	6.26	2.27	29.1	32.1	414,312	21,132	13,598 ± 694	–	0.85	N118E23
6A	975.7	73.7	44.23	6.26	2.27	17.2	24.7	463,710	20,942	19,805 ± 894	–	0.87	N22E4
6B	975.5	73.5	44.23	6.26	2.27	102.8	27.6	840,309	279,136	19,240 ± 6391	–	0.87	N21W12
7	975.1	73.1	44.23	6.26	2.27	20.6	38.9	518,890	23,489	15,334 ± 694	–	0.87	N171W33
8	969.3	67.3	44.23	6.26	2.26	32.6	32.2	397,913	24,537	15,229 ± 639	–	0.72	N151W37
9	966.8	64.8	44.23	6.26	2.25	17.5	38.2	451,597	21,698	15,810 ± 760	–	0.76	N170W68
10	959.8	57.8	44.23	6.26	2.24	23.6	37.2	321,967	15,754	9877 ± 483	–	0.84	N145W72
11	950.7	48.7	44.23	6.26	2.22	23.5	38.6	310,801	16,034	9791 ± 505	–	0.80	N77W72
12	944.0	42.0	44.23	6.26	2.21	22.3	37.4	298,013	15,522	11,668 ± 608	–	0.67	N14W72
13A	940.4	38.4	44.23	6.26	2.21	28.0	38.0	290,021	15,713	10,276 ± 556	–	0.71	N106W87
13B	940.4	38.4	44.23	6.26	2.21	43.3	38.4	257,546	22,005	8397 ± 717	–	0.71	N106W87
14	930.9	28.9	44.23	6.26	2.19	29.8	37.3	467,713	23,683	19,233 ± 974	–	0.65	N140E89
15	922.4	20.4	44.23	6.26	2.17	25.3	37.3	330,443	16,938	16,245 ± 833	–	0.55	N4E84
16	915.4	13.4	44.23	6.26	2.16	27.3	31.8	341,914	17,288	22,348 ± 1130	–	0.47	N162W26
17	911.6	9.6	44.23	6.26	2.16	22.9	37.7	229,307	13,073	13,660 ± 779	–	0.45	N13W71
18	908.2	6.2	44.23	6.26	2.15	29.0	38.0	396,966	22,406	25,803 ± 1456	–	0.43	N140W80
19	907.2	5.2	44.23	6.26	2.15	30.4	35.7	268,197	14,974	18,429 ± 1029	–	0.40	N179W61
20	905.4	3.4	44.23	6.26	2.14	28.8	33.2	98,729	8562	6581 ± 572	–	0.41	N0E84
21	904.5	2.5	44.23	6.26	1.49	21.2	37.5	26,219	3368	1267 ± 163	–	0.52	N155E83
22	903.6	1.6	44.23	6.26	1.49	22.6	37.4	17,964	3489	830 ± 161	–	0.53	N150E56

3.3. Topographic shielding estimation in a narrow gorge

The estimation of topographic shielding (TS) allows the calibration of the sampled surfaces exposure ages by evaluating how much cosmic rays were obstructed by the surrounding topography, which decreases the cosmogenic nuclides production rate (Dunne et al., 1999). The TS factor is defined as the ratio of the received cosmic flux at a given point over the maximum flux at this point assuming an unshielded exposure (Dunne et al., 1999; Gosse and Phillips, 2001). It is commonly calculated using the following equation from Dunne et al. (1999):

$$C_T = 1 - \frac{1}{2\pi} \sum_{i=1}^{n} \Delta\varnothing_i \sin^{m+1}(\theta_i)$$

where C_T is the TS factor, n is the number of topographic obstructions that are measured around a sampled surface, each obstruction being represented by a pair of azimuth $\varnothing_i$ and elevation angles θ_i, m is a constant which commonly cited value is 2.3 (Gosse and Phillips, 2001). This factor is commonly estimated in the field during surface sampling by measuring, using a compass, the horizon elevation at 360° around the sampled surface (Gosse and Phillips, 2001). However, such protocol is difficult to implement in gorges while sampling the vertical wall, and is complexified by the 3D geometry of the gorge.

Numerical methods exist to estimate TS from Digital Elevation Models (DEM), which have been demonstrated on basin-averaged denudation rate studies (e.g. Codilean, 2006; Balco et al., 2008). In this paper, we used the tools developed by Li (2013), for the GIS software ArcGis, using high-resolution DEMs of the CdB Gorge and its surrounding. The DEMs used are built from the Structure-from-Motion method, using aerial photographs acquired by plane, for the surrounding gorge topography, and UAV, for the mapping of the vertical parts (gorges walls), following an adaptation of the methodology presented in Vasquez-Tarrio et al. (2017).

The resulting data set has a resolution of 50 cm, with a precision of 2.6 m (RMSE), for the model surroundings used for the TS factor determination, and 7 cm with a precision of 16.8 cm (RMSE) for the DEM used for the mapping of the incision markers in the gorge. Such precision has been achieved in a vertical environment, without GPS signal, with the use of a total station (Leica TS02) for the acquisition of Ground

Control Point (GCP). The code by Li (2018) allows us to calculate the maximum elevation for each azimuth value (horizontal angle from 0° to 360° by 5° increment) around the sampled surface.

In a previous study, Norton and Vanacker (2009) mentioned that the use of a DEM with resolution lower than 5 m (5 m being the optimal resolution) can cause an overestimation of the TS factor, because of the ability of cosmic rays to pass through small obstructions without any significant interaction (Norton and Vanacker, 2009). However, in gorges, the use of a higher resolution DEM is required for the numerical determination of the TS factor, as the samples were all gathered in a narrow horizontal (XY) space, even if they lie at a larger distance from each other in the vertical Z dimension. Furthermore, the only obstructions in the gorge are the ≈200 m thick limestone walls. A precise estimate of TS is very important in the CdB Gorge, as it can have a large impact on the calculated CRE ages.

3.4. Denudation rates

Denudation, which includes mechanical and chemical erosion, is an important process in the shaping of carbonate landscapes (Ryb et al., 2014a, 2014b). The efficiency of the denudation process is controlled in part by the slope and convexity of the surfaces that are involved (Godard et al., 2016; Thomas et al., 2017). Gravitational processes must be considered, but also the spatial variability of the carbonate dissolution efficiency, which results from numerous slope morphological irregularities (overhangs, recesses, fractures). Because the radionuclide concentration at the surface results from a constant competition between surface denudation and production by exposure to cosmic rays, the denudation rate is an important factor that needs to be determined in order to calculate the CRE ages. In the SW Alps, a regional denudation rate of ≈30 mm/kyr has been estimated in the literature (e.g. Godard et al., 2016, 2020; Thomas et al., 2017), and this parameter has also been constrained locally for our site by using steady-state radionuclide concentrations. For this purpose, four sub-horizontal surfaces have been sampled on the top of the limestone bar in which the gorge was incised (≈250 m above riverbed) (Figs. 2C and 3A). The denudation rates are calculated assuming infinite time and scaling parameters mention in Section 3.2, after the procedure described Schimmelpfennig et al. (2009).

4. Results

4.1. Flat upper surface: steady-state denudation rates

Measured radionuclide concentrations (samples 1 to 4, Figs. 2C and 3A, ≈250 m above river) for the horizontal high hanging paleo-surface of the limestone bar range from 1.56 to 2.84 × 10^6 ^{36}Cl at/g (Table 1). Assuming these samples at steady-state (i.e. their exposure time is long enough to ensure that concentrations have reached a plateau) yields to steady-state denudation rates ranging between 18.74 ± 1.05 and 32.54 ± 1.76 mm/ka for these top samples. These values are in agreement with previous estimates (e.g. Godard et al., 2016, 2020; Thomas et al., 2017; Siame et al., 2004; Zerathe et al., 2014), for the SW Alps.

4.2. Gorge steep slope/middle part: rockfall markers

4.2.1. Fracturation

The CdB Gorge walls are heavily fractured and prone to rock mass movements, as observed by our field structural analysis: two major fracture families have been measured on the gorge walls, both trending N30°E (i.e., parallel to the gorge strike), the first one dipping ~70°W and the second one dipping 40–50°E, while the bedding is ~EW and vertical (Fig. 4).

4.2.2. CRE age

Denudation rates obtained on horizontal surfaces do not reflect the true denudation that has affected the vertical walls of the gorge. Indeed, it is generally considered that vertical and sub-vertical surfaces undergo less dissolution than gently dipping or horizontal surfaces, as they receive much less water runoff, and water does not stagnate or percolate (Sadier et al., 2012). Compiling denudation rates determined from our data and those from literature, we have decided to consider a denudation rate of 10 mm/ka for vertical or sub-vertical surfaces, following Sadier et al. (2012). CRE ages determined from ^{36}Cl concentrations are reported in the age-elevation plots (Fig. 5A). The profile displays ages between 22 and 8 ka We can observe two ages clusters, one at ≈17 ka (samples 5 to 9) and the other one at ≈10 ka (samples 10 to 13A), respectively.

As shown in Fig. 5A, the CRE ages distribution does not correlate with the altitude of the samples and especially, we do not see any systematic rejuvenation of the CRE ages towards the base of the gorge at the current riverbed level, as it can be expected for a gorge slope affected by post-incision erosion processes (such as rockfall or dissolution). The interpretation of these ages therefore requires a more detailed analysis taking into account the 3D morphology of the gorge walls, and the processes that may have affected the history of their exposure to cosmic rays.

4.3. River polished vertical surface/lower part: fluvial incision

CRE ages determined from the ^{36}Cl concentrations in the gorge lower part are reported in the age-elevation plots (Fig. 5B). The five samples (18 to 22) display ages between 25 ka and 800 a (Table 1). From these ages, we can compute two distinct incision rates: 0.15 mm/yr, from 25 ka to 2 ka, and 1.97 mm/yr, from 2 ka to present day, assuming a y-intercept equal to zero.

5. Discussion

5.1. Geomorphological interpretation of the CRE ages

Field and DEM observations evidence that the CdB Gorge walls have been rejuvenated several times in the middle part of the sampling profile (samples 5 to 17).

Actually, detailed field structural investigations of the gorge (Fig. 4) and DEM-based morphological analysis of the sampled wall (Fig. 6A, B, C) attest of such gravitational processes in the CdB Gorge. All the planes
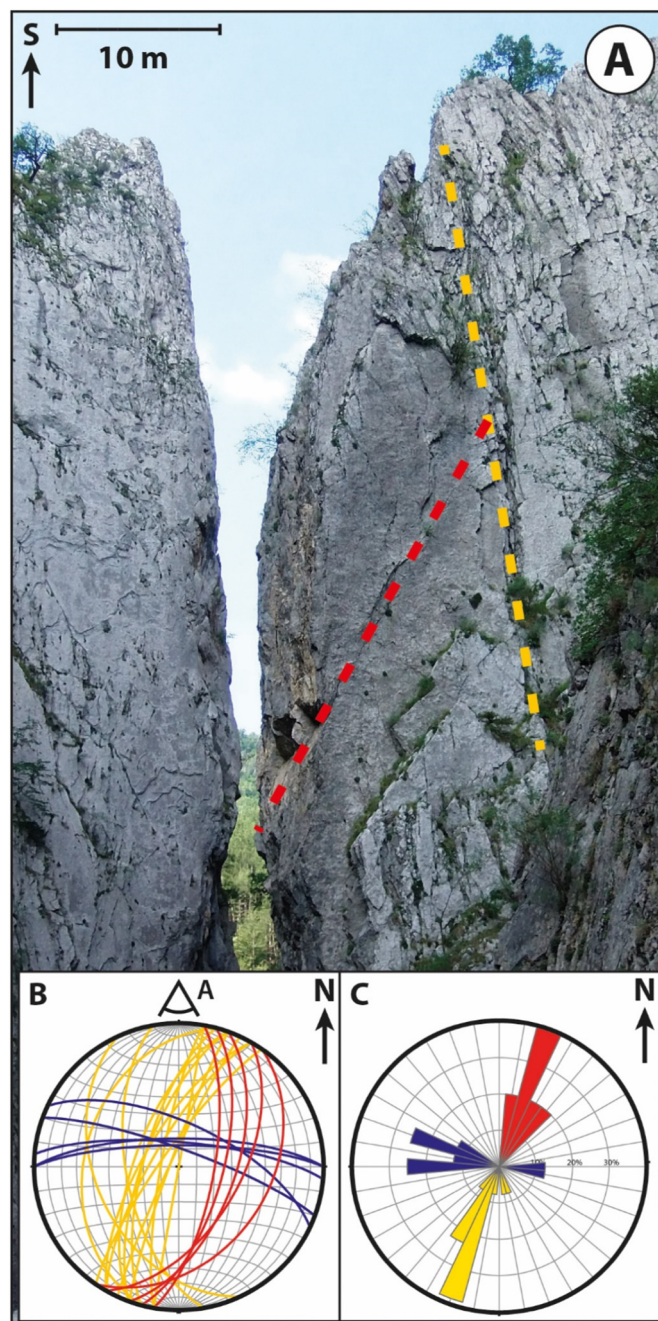

Fig. 4. A, West flank of CdB Gorge viewed towards the south with the two major representative fracture planes highlighted by red and yellow dashed lines. B, Projection of bedding plane (in blue), major fracture planes visible in A (red and yellow), Wulff projection, lower hemisphere. C, Rose diagram of bedding and fracture planes (same colors).

(fractures and bedding) described in previous Section 4.2 (Fig. 4) can play a role in the occurrence of rockfall events by isolating polygonal blocks susceptible to fall from the rock scarp. Furthermore, differential erosion between the various vertical limestone strata of different thickness, ranging from ≈20 m to >1 m, destabilizes the vertical walls and thus leads more competent strata to be in an unstable overhanging position. These observations highlight the predisposing factors and vulnerability of the gorge to rockfall hazard. The combination of vertical incision and lateral gravitational processes can therefore explain the peculiar V-profile of the CdB Gorge.

The main fracture orientations (yellow; Figs. 4 and 6A, B, C), are parallel to the surface of the profile in its middle part (from samples 7 to 12; Fig. 6C) suggesting that this surface may result from rockfall events. The
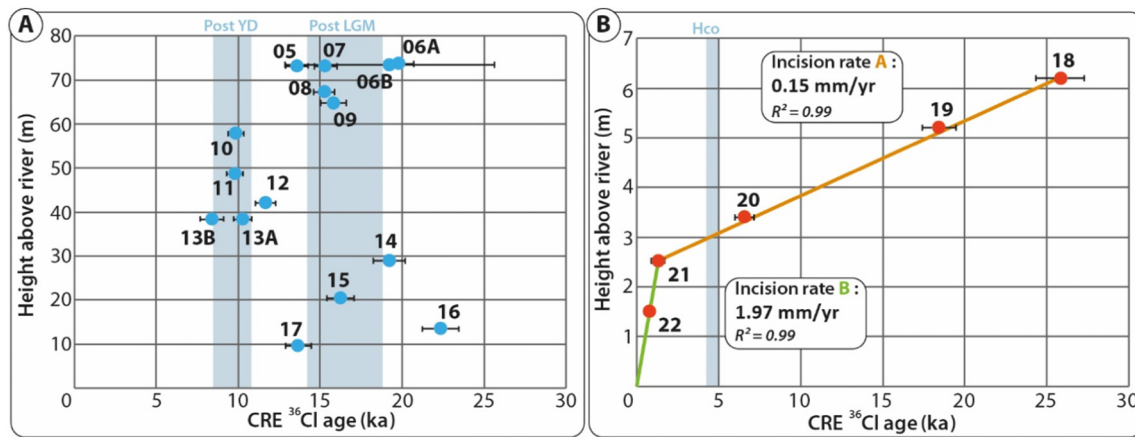
Fig. 5. Height above river bed versus exposure age, determined by [36]Cl concentration, for the 18 dated samples collected in the middle (A) and lower part (B) of the CdB Gorge. The dot colors are in reference to Fig. 3: the red dots refer to the river polished lower part, and the blue dots refer to the middle part of profile. With the five CRE ages ascribed to the fluvial incision process (B), we are able to compute incision rates ranging from 0.15 mm/yr to 1.97 mm/yr, which might suggest an acceleration of incision after 2 ka. Known deglaciation periods are chronologically represented by light blue columns: post LGM (Last Glacial Maximum): ≈19–14 ka Clark et al. (2009); Post YD (Post Younger Dryas): ≈11–8 ka Darnault et al. (2012); Hco (Holocene climatic optimum): ≈5–4 ka; Zerathe et al. (2014).

fracture pattern and the morphology of the wall suggest the toppling of a large vertical column (≈20 m high; Fig. 6D), prepared by joints opened within the vertical limestone beds. Following this observation and the CRE ages, it appears that the column was toppled by two distinct events, involving first the upper part of the column (samples 7 to 9) and then its lower part (samples 10 to 12) at ≈17 ka and ≈10 ka respectively (Fig. 5A). Other sampled surfaces, from samples 5 to 6B and 13A to 17, show an age distribution with three clusters ranging from 14.5 to 22 ka, from 10 to 30 m above riverbed. The age versus height distribution does not show any clear trend, which suggests that these surfaces were later rejuvenated by gravitational processes.

Finally, in the lower part of the profile, the linear decrease of CRE ages towards the riverbed is suggestive of fluvial incision, which can be separated into two phases: i) from sample 18 to 21 (0.15 mm/yr), and ii) from sample 21 to riverbed (2.15 mm/yr). However, the latter incision rate only concerns the foot of the gorge wall (>2.5 m high) which can be rejuvenated by punctual and recent flood events, and is constrained by only two points (three if we take into account the (0,0) point corresponding to riverbed). Hence, the estimated incision rate of 2.15 mm/yr is not representative of the long-term fluvial incision process that is responsible for the formation of the CdB Gorge.

5.2. Climatic control on gravitational events

Major rockfall events can be interpreted as the result of changing climate conditions, as these processes are well known to be sensitive to permafrost degradation during warming phases (e.g. Ravanel et al., 2010; Hilger et al., 2021). Based on our case example, these gravitational processes appear to be an important factor of the gorge erosion. We obtained two age clusters which we interpret as two instantaneous rockfall events having occurred at ≈17 and ≈10 ka respectively. These ages correspond to the two last major deglaciation phases: post LGM (≈19–14 ka; Clark et al., 2009) and post Younger Dryas (≈11–8 ka; Darnault et al., 2012) (Fig. 5). Although reconstructions of permafrost are still lacking for this period of time, we suggest that this relatively high-altitude area could have been under permafrost influence, due to its elevation above the equilibrium line altitude for glaciers during the LGM and Younger Dryas, and its proximity to the glacier front (Brisset et al., 2015 and references therein). Therefore, these gravitational events could have been caused by permafrost degradation, adding to a potential increase of freezing and thawing cycles during glacial phases (Sanchez et al., 2010; Lebrouc et al., 2013; Hilger et al., 2021). These observations therefore suggest that the CdB Gorge formation results from

a vertical fluvial incision process, and is later widened by glacial and postglacial processes related to climate phases.

5.3. Regional comparison of river incision rates in SW Alps and possible controlling factors: climate, fluvial regime and surface uplift

Several studies based on CRE dating have been carried out on gorges and valleys of the SW Alps (Saillard et al., 2014; Rolland et al., 2017; Petit et al., 2019; Fig. 7). The comparison of fluvial incision at the scale of SW Alps from gorges formed in valleys with or without glacial influence shows the dominance of high and variable incision rates in formerly glaciated catchments, while catchments devoid of glacial influence have lower incision rates since the LGM. Indeed, glaciated areas accumulate topographic disequilibrium during glaciation (Brocard and van der Beek, 2006). Readjustments after glacial perturbations imply enhanced erosion by fluvial and hillslopes processes, especially during deglaciation (Norton et al., 2010; Fox et al., 2015). In catchments dominated by glaciers during the LGM and Younger Dryas in their higher parts, the above authors determined incision rates ranging from 1 mm/yr to ≈8 mm/yr (Fig. 7 and C). The most extreme values are restricted to the catchments higher altitude (>900 m) and can be attributed to transient incision of late glacial morphologies after the Younger Dryas (Rolland et al., 2017). In formerly glaciated areas, the post-LGM incision might be controlled by climatic variations, through punctual post-glacial outbursts, and topographic readjustment through transient headward erosion. Therefore, these locally very high incision rates cannot be used to infer any long-term tendency.

Out of the influence of glaciers, the incision rates estimated for the Estéron River (Petit et al., 2019) and the Bès River (this study) are of ≈1.0 and 0.15 mm/yr respectively (Fig. 7; Petit et al., 2019; this study). However, if we compare incision rates between the Vésubie, Estéron and Bès rivers after the last cold climatic event (i.e., the Younger Dryas), despite the fact that all three profiles are measured in a similar lithology and under comparable climatic settings, the mean incision rate of the Bès river (0.15 mm/yr) appears significantly lower than in the Vésubie (2.0 ± 0.1 mm/yr), like for all catchments with glacial influence. In comparison to a catchment positioned in a similar glacier-free setting, the Esteron River (1.0 ± 0.1 mm/yr), the river incision rate value estimated for the Bès is still significantly lower.

Surface uplift, which is a combination of isostatic rebound, tectonic uplift and erosion, may also cause incision rate variability (e.g. Kirby and Whipple, 2012). Isostatic rebound, either induced by Quaternary erosion and LGM glacier retreat, has been shown to be insignificant in
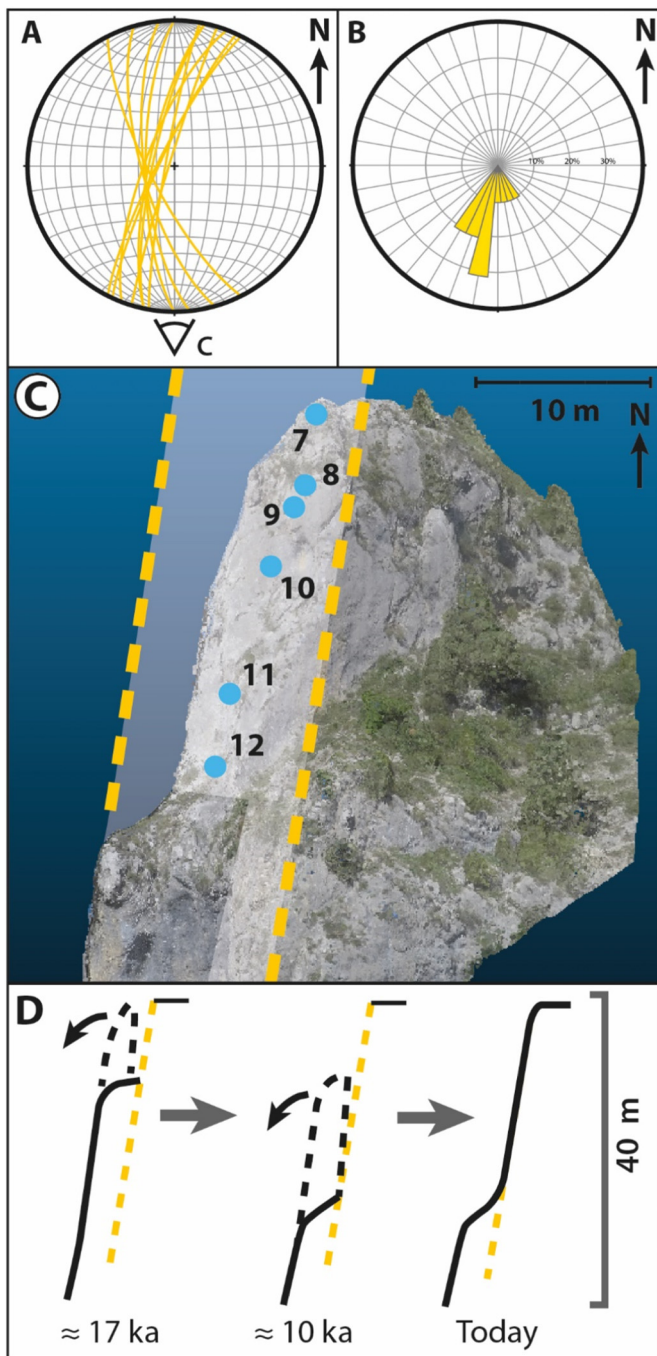
Fig. 6. Geometrical characteristics of the rockfall domain in the middle part of the CdB Gorge profile. A-B, Dip and strike measurements of the sample profile upper part (calculated from the DEM) in a Wulff stereographic projection, lower hemisphere (A) and in a Rose diagram (B). C, Mean plane deduced from the DEM calculated strike and dip of the upper sampled surface (yellow dashed framed rectangle) and location of the rejuvenated samples (samples 7 to 12; blue dots). D. Interpretation of the rockfall process by toppling that may have caused the rejuvenation of the sampled surface.

the SW Alps (Champagnac et al., 2007; Norton and Hampel, 2010; Sternai et al., 2019). Regarding the tectonic uplift component, cooling rates from Apatite Fission Track measurements in the external crystalline massif of the Argentera-Mercantour (Bogdanoff et al., 2000; Bigot-Cormier et al., 2006) lead to long-term exhumation rates of 1.1– 1.4 mm/yr (rock uplift) over the last 10 Myr. Closer to our study area, Schwartz et al. (2017) demonstrated by low-temperature thermochronometry that the Barles erosional half-window area has

been exhuming at a long-term rate of $\approx$0.7 mm/yr since 5 Ma. Recent studies using GPS monitoring in the Alps (Walpersdorf et al., 2018; Sternai et al., 2019) evidence a present-day surface uplift rate of 0.5 to 1 mm/yr in the highest parts of the Alpine massifs, while GPS stations closer to our study area (La Javie and Moustiers-Sainte-Marie) have short-term uplift rates of 0.025 ± 0.9 and -0.41 ± 0.58 mm/yr, respectively (Sternai et al., 2019).

Hence, the relatively high incision rates recorded in the Var catchment and tributaries compared to the slow rate determined at the CdB Gorge may reflect the east to west (i.e. massifs highest parts to Alpine foreland) regional variability of both long-term and short-term uplift rates. Nevertheless, in order to better discriminate the respective role of local catchment dynamics (glacial or not) and uplift rates variability on fluvial incision process, further constraints on incision rates are needed at the scale of SW Alps.

6. Conclusion

We sampled and measured in situ-produced ^{36}Cl concentrations in twenty Jurassic limestone samples along a 80 m high sub-vertical and continuous profile of the V-shaped CdB Gorge (SW Alps) and in four samples collected at the top of the Jurassic limestone bar in which the CdB Gorge is incised. High-resolution DEM analysis and CRE ages show that the CdB Gorge was first dug by fluvial incision and subsequently widened by secondary gravitational processes. The top four samples are suggestive of a steady-state ^{36}Cl concentration that allows quantifying a denudation rate between 18 and 33 mm/kyr in the flatter upper, perfectly exposed surfaces on the shoulders of the gorge. CRE ages of the 10 m above riverbed profile allow quantifying a mean fluvial incision rate of 0.15 mm/yr over the last 25 ka, with an acceleration up to 2 mm/yr for the last 2 ka that can be linked to extreme flood events. The comparison of CRE dating results at the scale of SW Alps shows that the fluvial incision of Bès River is significantly lower than in other basins, which is ascribed to its frontal position in the Alps and glacier-free watershed during glacial phases. Moreover, CRE ages obtained in the middle part of the gorge are suggestive of two main rockfall events, which occurred $\approx$17 ka and $\approx$10 ka ago. These two events correspond to deglacial stages of the LGM and Younger Dryas, respectively, while their geometry suggests debuttressing along two recognized fracture families. These data suggest the triggering of rockfalls in a warming climate during paraglacial episodes. More sporadic rockfalls may explain age variability in the profile middle part. Based on this example, fluvial gorges in periglacial settings could be efficiently shaped by rockfalls during deglaciation periods, once fluvial incision has exposed the walls.

Declaration of competing interest

The authors declare that they have no known competing financial interests or personal relationships that could have appeared to influence the work reported in this paper.
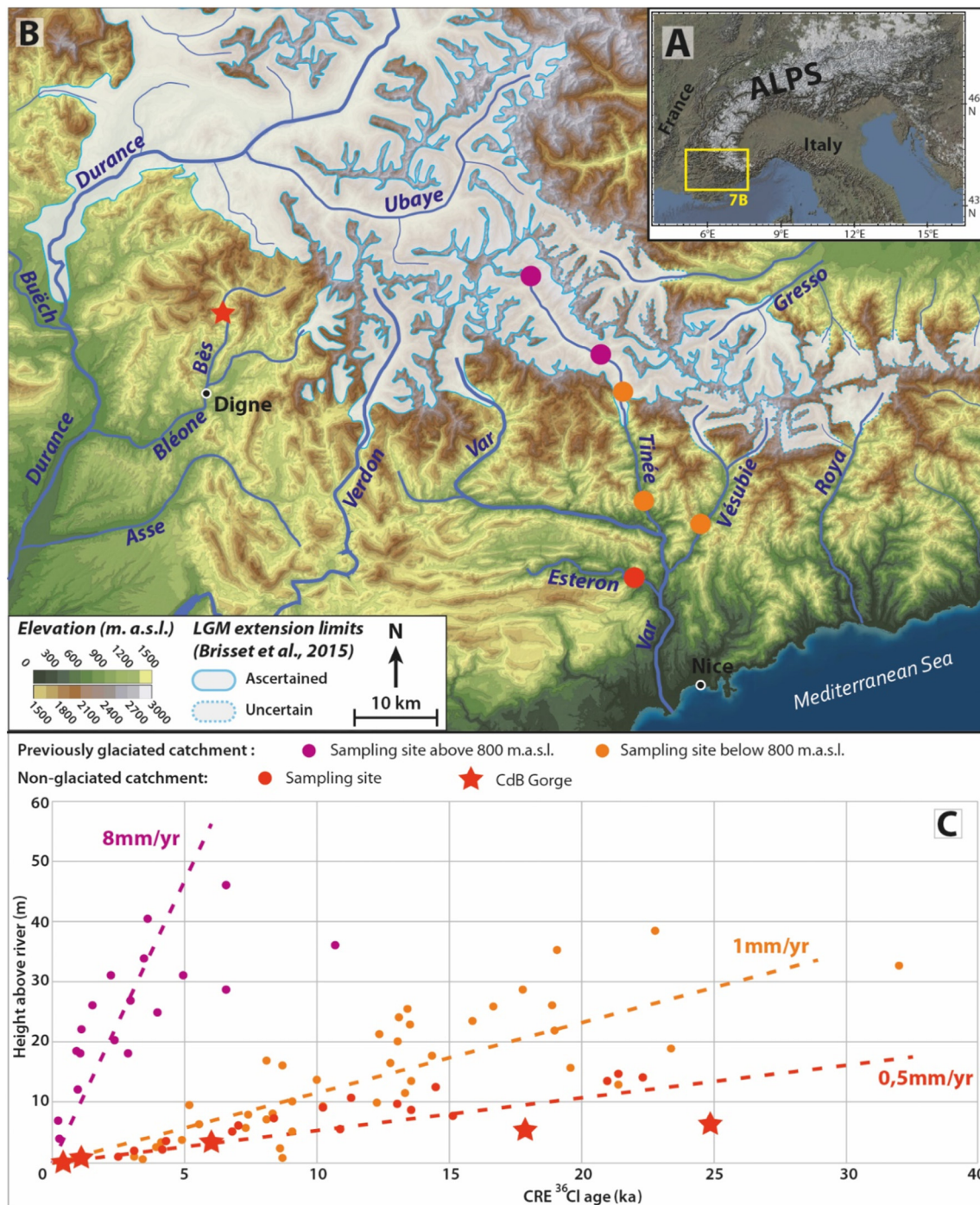
Acknowledgments

Fig. 7. A, Location of study area in the European Alps. B, Location of the CdB Gorge from this study and previous ones (Saillard et al., 2014; Petit et al., 2019; Rolland et al., 2017) in the SW Alps set against the Last Glacial Maximum (LGM) extension limits (modified from Brisset et al., 2015). Note that the glaciated/non-glaciated specification refers to the glaciation of the catchment during the LGM, and not the sampling site itself. C, Comparison of incision rate determined by CRE dating from this study (red stars) and previous ones (Saillard et al., 2014; Petit et al., 2019; Rolland et al., 2017). Note the increase of site specific incision rate according to their altitude and location in regard of the LGM extension limits.

References

Adams, J., 1985. Large-scale tectonic geomorphology of the Southern Alps, New Zealand. In: Morisawa, M., Hack, J.T. (Eds.), Tectonic Geomorphology. Allen and Unwin, Boston, pp. 105–128.

Arnold, M., Merchel, S., Bourlès, D.L., Braucher, R., Benedetti, L., Finkel, R.C., Aumaître, G., Gottdang, A., Klein, M., 2010. The French accelerator mass spectrometry facility ASTER: improved performance and developments. Nucl. Inst. Methods Phys. Res. B 268, 1954–1959.

Bacon, S.N., McDonald, E.V., Caldwell, T.G., Dalldorf, G.K., 2009. Timing and distribution of alluvial fan sedimentation in response to strengthening of late Holocene ENSO variability in the Sonoran Desert, southwestern Arizona, USA. Quat. Res. 73, 425–438.

Balco, G., Stone, J.O., Lifton, N.A., Dunai, T.J., 2008. A complete and easily accesible means of caltulating surfaces exposure ages or erosion rates from ^{10}Be and ^{26}Al measurements. Quat. Geochronol. 3, 174–195.

Bigot-Cormier, Sosson M., Poupeau, G., Stéphan, J.-F., Labrin, E., 2006. The denudation history of the Argentera Alpine External Crystalline Massif (Western Alps, France-Italy): an overview from the analysis of fision tracks in apatites and zircons. Geodin. Acta 19 (6), 455–473.

Bogdanoff, S., Michard, A., Mansour, M., Poupeau, G., 2000. Apatite fission track analysis in the Argentera massif: evidence of contrasting denudation rates in the External Crystalline Massifs of the Western Alps. Terra Nova 12, 117–125.

Braucher, R., Merchel, S., Borgomano, J., Bourlès, D.L., 2011. Production of cosmogenic radionuclides at great depth: a multi element approach. Earth Planet. Sci. Lett. 309, 1–9.

Braucher, R., Keddadouche, K., Aumaître, G., Bourlès, D.L., Arnold, M., Pivot, S., Baroni, M., Scharf, A., Rugel, G., Bard, E., 2018. Chlorine measurements at the 5 MV French AMS national facility ASTER: associated external uncertainties and comparability with the 6MV DREAMS facility. Nuclear Inst, and Methods in Physics Research, B 420, 40–45.

Brisset, E., Guiter, F., Miramont, C., Revel, M., Anthony, E.J., Belhon, C., Arnaud, F., Malet, E., de Beaulieu, J.-L., 2015. Lateglacial/Holocene environmental changes in the Mediterranean Alps inferred from lacustrine sediments. Quaternary Sci. Rev. 110, 49–71.

Brocard, G., van der Beek, P., 2006. Influence of incision rate, rock strength, and bedload supply on bedrock river gradients and valley-flat widths: Field-based evidence and calibrations from western Alpine rivers (southeast France). Geological Society of America 398, 101–126.

Brocard, G.Y., Van Der Beek, P., Bourlès, D., Siame, L., Mugnier, J.-L., 2003. Long-term fluvial incision rate and postglacial river relaxation time in the French Western Alps from ^{10}Be dating of alluvial terraces with assessment of inheritance, soil developpement and wind ablations effects. Earth Planet. Sci. Lett. 209, 197–214.

Brocklehurst, S.H., Whipple, K.X., 2002. Glacial erosion and relief production in the Eastern Sierra Nevada, California. Geomorphology 42, 1–24.

Champagnac, J.D., Molnar, P., Anderson, R.S., Sue, C., Delacou, B., 2007. Quaternary erosion-induced isostatic rebound in the western Alps. Geol. Soc. Am. Bull. 35 (3), 195–198.

Champagnac, J.D., van der Beek, P., Diraison, G., Dauphin, S., 2008. Flexural isostatic response of the Alps to increased Quaternary erosion recorded by foreland basin remnants, SE France. Terra Nova 20, 213–220.

Clark, P.U., Dyke, A.S., Shakun, J.D., Carlson, A.E., Clark, J., Wohlfarth, B., Mitrovica, J.X., Hostetler, S.W., McCabe, A.M., 2009. The Last Glacial Maximum. Science 325, 710–714.

Codilean, A.T., 2006. Calculation of the cosmogenic nuclide production topographic shielding sclaning factor for large areas using DEMs. Earth Surf. Proc. Land 31 (6), 785–794.

Darnault, R., Rolland, R., Rolland, Y., Bourlès, D., Revel, M., Sanchez, G., Bouissou, S., 2012. Timing of the last deglaciation revealed by receding glaciers at the Alpine-scale: impact on mountain geomorphology. Quaternary Sci. Rev. 3, 127–142.

Delacou, B., Sue, C., Champagnac, J.-D., Burkhard, M., 2004. Present-say geodynamics in the bend of the western and central Alps as constrained by earthquake analysis. Geophys. J. Int. 158, 753–774.

Dumont, T., Schwartz, S., Guillot, S., Simon-Labric, T., Tricart, P., Jourdan, S., 2012. Structural and sedimentary records of the Oligocene revolution in the Western Alpine arc. J. Geodyn. 56-57, 18–38.

Dunne, J., Elmore, D., Muzikar, P., 1999. Scaling factors for the rates of production of cosmogenic nuclides for geometric shielding and attenuation at depth on sloped surfaces. Geomorphology 27, 3–11.

England, P., Molnar, P., 1990. Surface uplift, uplift of rocks, and exhumation of rocks. Geology 18, 1173–1177.

Fox, M., Leith, K., Bodin, T., Balco, G., Shuster, D.L., 2015. Rate of fluvial incision in the Central Alps constrained throught joint inversion of detrital 10Be and thermochronometric data. Earth Planet. Sci. Lett. 411, 27–36.

Godard, V., Ollivier, V., Bellier, O., Miramont, C., Shabanian, E., Fleury, J., Benedetti, L., Guillou, V., ASTER Team, 2016. Weathering-limited hillslope evolution in carbonate landscapes. Earth Planet. Sci. Lett. 446, 10–20.

Godard, V., Hippolyte, J.-C., Cushing, E., Espurt, N., Fleury, J., Bellier, O., Ollivier, V., ASTER Team, 2020. Hillslope denudation and morphologic response across a rock uplift gradient. Earth Surf. Dynam. 8, 221–243.

Gosse, J., Phillips, F., 2001. Terrestrial in situ cosmogenic nuclides: theory and application. Quaternary Sci. Rev. 20, 1475–1560.

Hilger, P., Hermanns, R.L., Czekirda, J., Myhra, K.S., Gosse, J.C., Etzelmüller, B., 2021. Permafrost as a first order control on long-term rock-slope deformation in (Sub-) Arctic Norway. Quat. Sci. Rev. 251, 106718.

Hippolyte, J.-C., Dumont, T., 2000. Identification of Quaternary thrusts folds and faults in a low seismicity area: examples in the Southern Alps (France). Terra Nova 12, 156–162.

Kirby, E., Whipple, K.X., 2012. Expression of active tectonics in erosional landscapes. J. Struct. Geol. 44, 54–75.

Korup, O., Schlunegger, F., 2007. Bedrock landsliding, river incision, and transience of geomorphic hillslope-channel coupling: evidence from inner gorges in the Swiss Alps. J. Geophys. Res. 112, F03027.

Lal, D., 1991. Cosmic ray labeling of erosion surfaces: in situ nuclide production rates and erosion models. Earth Planet. Sci. Lett. 104, 424–439.

Lavé, J., Avouac, J.P., 2001. Fluvial incision and tectonic uplift across the Himalayas of central Nepal. J. Geophys. Res. 106 (B1), 25561–25593.

Lebrouc, V., Schwartz, S., Baillet, L., Jongmans, D., Gamond, J.F., 2013. Permafrost extension modeling in a rock slope since the Last Glacial Maximum: application to the large Séchilienne landslide (French Alps). Geomorphology 198, 189–200.

Li, Y.-K., 2013. Determining topographic shielding from digital elevation models for cosmogenic nuclide analysis: a GIS approach and field validation. J. Mt. Sci. 10 (3), 355–362.

Li Y.-K., 2018. Determining topographic shielding from digital elevation models for cosmogenic nuclide analysis: a GIS model for discrete sample sites. J. Mt. Sci., 15, 5 939–947.

Merchel, S., Bremser, W., Alfimov, V., Arnold, M., Aumaître, G., Benedetti, L., Bourlès, D.L., Caffee, M., Fifield, L.K., Finkel, R.C., Freeman, S.P.H.T., Martschini, M., Matsushi, Y., Rood, D.H., Sasa, K., Steier, P., Takahashi, T., Tamari, M., Tims, S.G., Tosaki, Y.,

Wilcken, K.M., Xu, S., 2011. Ultra-trace analysis of 36Cl by accelerator mass spectrometry: an interlaboratory study. Anal. Bioanal. Chem. 400, 3125–3132.

Montgomery, D.R., 2002. Valley formation by fluvial and glacial erosion. Geology 30, 1047–1050.

Montgomery, D.R., Korup, O., 2010. Preservation of inner gorges through repeated Alpine glaciations. Nat. Geosci. 4, 62–67.

Nocquet, J.-M., Sue, C., Walpersdorf, A., Tran, T., Lenôtre, N., Vernant, P., Cushing, M., Jouanne, F., Masson, F., Baize, S., Chéry, J., van der Beek, P.A., 2016. Present-day uplift of the western Alps. Sci. Rep. 6, 28404.

Norton, K.P., Hampel, A., 2010. Postglacial rebound promotes glacial re-advances – a case study from the European Alps. Terra Nova 22, 297–302.

Norton, K.P., Vanacker, V., 2009. Effects of terrain smoothing on topographic shielding correction factors for cosmogenic nuclide-derived estimates of basin-averaged denudation rates. Earth Surf. Proc. Land 34, 145–154.

Norton, K.P., Abbühl, L.M., Schlunegger, F., 2010. Glacial conditioning as an erosional driving force in the Cenral Alps. Geology 38 (7), 655–658.

Ouimet, W.B., Whipple, K.X., Crosby, B.T., Johnson, J.P., Schildgen, T.F., 2008. Epigenetic gorges in fluvial landscapes. Earth Surf. Proc. Land 33 (13), 1993–2009.

Pan, B., Burbank, D.W., Wang, Y., Wu, G., Li, J., Guan, Q., 2003. A 900 k.y. Record of strath terrace formation during glacial-interglacial transitions in northwest China. Geology 31, 957–960.

Pazzaglia, F.J., Gardner, T.W., Merritts, D.J., 1998. Bedrock fluvial incision and longitudinal profile development over geological time scales determined by fluvial terraces. In: Wohl, E., Tinkler, K. (Eds.), Bedrock Channels. Geophysical Monograph Series vol. 107. American Geophysical Union, Washington, pp. 207–235.

Petit, C., Goren, L., Rolland, Y., Bourlès, D., Braucher, R., Saillard, M., Cassol, D., 2017. Recent, climate-driven river incision rate fluctuations in the Mercantour crystalline massif, southern French Alps. Quaternary Sci. Rev. 165, 73–87.

Petit, C., Rolland, Y., Braucher, R., Bourlès, D., Guillou, V., Petitperrin, V., 2019. River incision and migration deduced from ^{36}Cl cosmic-ray exposure durations: the Clue de la Cerise gorge in southern French Alps. Geomorphology 330, 81–88.

Pratt, B., Burbank, D.W., Heimsath, A., Ojha, T., 2002. Impulsive alluviation during early Holocene strengthened monsoons, central Nepal Himalaya. Geology 30 (10), 911–914.

Ravanel, L., Allignol, F., Deline, P., Gruber, S., Ravello, M., 2010. Rockfalls in the Mont Blanc Massif in 2007 and 2008. Landslides 7 (4), 493–501.

Rolland, Y., Petit, C., Saillard, M., Braucher, R., Bourlès, D., Darnault, R., Cassol, D., ASTER Team, 2017. Inner gorges incision history: a proxy for deglaciation? Insights from Cosmic Ray Exposure dating (^{10}Be and ^{36}Cl) of river-polished surfaces (Tinée River, SW Alps, France). Earth Planet. Sci. Lett. 457, 271–281.

Ryb, U., Matmon, A., Erel, Y., Haviv, I., Katz, A., Starinsky, A., Angert, A., ASTER Team, 2014a. Controls on denudation rates in tectonically stable Mediterranean carbonate terrain. The Geol. Soc. Am. Bull. Bulletin 126, 553–568.

Ryb, U., Matmon, A., Erel, Y., Haviv, I., Benedetti, L., Hidy, A.J., 2014b. Styles and rates of long-term denudation in carbonate terrains under a Mediterranean to hyper-arid climatic gradient. Earth Planet. Sci. Lett. 406, 142–152.

Sadier, B., Delannoy, J.-J., Benedetti, L., Bourlès, D.L., Jaillet, S., Geneste, J.-M., Lebatard, A.-E., Arnold, M., 2012. Further constraints on the Chauvet cave artwork elaboration. Proc. Natl. Acad. Sci. U. S. A. 109, 8002–8006.

Saillard, M., Petit, C., Rolland, Y., Braucher, R., Bourlès, D.L., Zerathe, S., Revel, M., Jourdon, A., 2014. Late Quaternary incision rates in the Vésubie catchment area (Southern French Alps) from in situ-produced ^{36}Cl cosmogenic nuclide dating: tectonic and climatic implications. J. Geophys. Res. Earth Surf. 119, 1121–1135.

Sanchez, G., Rolland, Y., Corsini, M., Braucher, R., Bourlès, D., Arnold, M., Aumaître, G., 2010. Relationships between tectonics, slope instability and climate change: Cosmic Ray exposure dating of active faults, landslides and glacial surfaces in the SW Alps. Geomorphology 107 (1–2), 1–13.

Schaller, M., Hovius, N., Willett, S.D., Ivy-Ochs, S., Synal, H.-A., Chen, M.-C., 2005. Fluvial bedrock incision in the active mountain belt of Taiwan from in situ-produced cosmogenic nuclides. Earth Surf. Proc. Land 30, 955–971.

Schimmelpfennig, I., Benedetti, L., Finkel, R., Pik, R., Blard, P.-H., Bourlès, D.L., Burnard, P., Williams, A., 2009. Source of in situ ^{36}Cl in basaltics rocks. Implication for calibration of production rates. Quat. Geochronol. 4, 441–461.

Schwartz, S., Gautheron, C., Audin, L., Dumont, T., Nomade, J., Barbarand, J., Pinna-Jamme, R., van der Beek P, 2017. Foreland exhumation controlled by crustal thickening in the Western Alps. Geology 45 (2), 139–142.

Serpelloni, E., Faccenna, C., Spada, G., Dong, D., Williams, S.D.P., 2013. Vertical GPS ground motion rates in the Euro-Mediterranean region: new evidence of velocity gradients at different spatial scales along the Nubia-Eurasia plate boundary. J. Geophys. Res. Solid Earth 118, 6003–6024.

Siame, L., Bellier, O., Braucher, R., Sébrier, M., Cushing, M., Bourlès, D., Hamelin, B., Baroux, E., de Voogd, B., Raisbeck, G., Yiou, F., 2004. Local erosion rates versus active tectonics: cosmic ray exposure modelling in Provence (south-east France). Earth Planet. Sci. Lett. 220, 345–364.

Sternai, P., Sue, C., Husson, L., Serpelloni, E., Becker, T.W., Willet, S.D., Faccenna, C., Giulio, A.D., Spada, G., Jolivet, L., Valla, P., Petit, C., Nocquet, J.-M., Walpersdorf, A., Castelletort, S., 2019. Present-day uplift of the European Alps: evaluating mechanisms and models of their relative contributions. Earth-Sci. Rev. 190, 589–604.

Stone, J.O., 2000. Air pressure and cosmogenic isotope production. J. Geophys. Res. Solid Earth 105, 23753–23759.

Sue, C., Delacou, B., Champagnac, J.-D., Allanic, C., Burkhard, 2007. Aseismic deformation in the Alps: GPS vs. seismic strain quantification. Terra Nova 1, 182–188.

Thomas, F., Godard, V., Bellier, O., Shabanian, E., Ollivier, V., Benedetti, L., Rizza, M., Espurt, N., Guillou, V., Hollender, F., Molliex, S., ASTER Team, 2017. Morphological controls on the dynamics of carbonate landscapes under a mediterranean climate. Terra Nova 29 (3), 173–182.

Valla, P.G., van der Beek, P.A., Carcaillet, J., 2010. Dating bedrock gorge incision in the French Western Alps (Ecrin-Pelvoux massif) using cosmogenic [10]Be. Terra Nova 22, 18–25.

Valla, P.G., Shuster, D.L., van der Beek, P.A., 2011. Significant increase in relief of the European Alps during mid-Pleistocene glaciations. Nat. Geosci. 4, 688–692.

Van der Woerd, J., Tapponnier, P., Ryerson, F.J., Meriaux, A.-S., Meyer, B., Gaudemer, Y., Finkel, R.C., Caffee, M.W., Zhao, G., Xu, Z., 2002. Uniform postglacial slip-rate along the central 600 km of the Kunlun Fault (Tibet), from [26]Al, [10]Be, and ^{14}C dating of riser offsets, and climatic origin of the regional morphology. Geophys. J. Int. 148, 356–388.

Vasquez-Tarrio, D., Borgniet, L., Liébault, F., Recking, A., 2017. Using UAS optical imagery and SfM photogrammetry to characterize the surface grain size of gravel bars in a braided river (Vénéon River, French Alps). Geomorphology 285, 94–105.

Walpersdorf, A., Pinget, L., Vernant, O., Sue, C., Deprez, A., RENAG team, 2018. Does long-term GPS in the Western Alps finally confirm earthquake mechanisms? Tectonics 37, 3721–3737.

Whipple, K.X., Kirby, E., Brocklehurst, S.H., 1999. Geomorphic limits to climate-induced increases in topographic relief. Nature 401, 39–43.

Wobus, C., Whipple, K.X., Kirby, E., Snyder, N., Johnson, J., Spaopolou, K., Crosby, B., Sheehan, D., 2006. Tectonics from topography: procedures, promise, and pit-falls. In: Willett, S.D., Hovius, N., Brandon, M.T., Fisher, D.M. (Eds.), Tectonics, Climate, and Landscape Evolution. Geol. Soc. Am. Bull. Special Paper vol. 398, pp. 55–74.

Zerathe, S., Lebourg, T., Braucher, R., Bourlès, D., 2014. Mid-Holocene cluster of larger-scale landslides revealed in the Southwestern Alps by [36]Cl dating. Insight on an Alpine-Scale landslide activity. Quaternary Sci. Rev. 90, 106–127.